High-permittivity core/shell stuctured NiO-based ceramics and their dielectric response mechanism

Yuanhua Lin, Lei Jiang, Rongjuan Zhao, and Ce-Wen Nan
State Key Laboratory of New Ceramics and Fine Processing, Department of Materials Science and Engineering, Tsinghua University, Beijing, 100084, P. R. China
(Received 4 January 2005; published 1 July 2005)

High-permittivity dielectric core/shell structured NiO-based ceramics (LSNO) have been successfully prepared. All the LSNO ceramic samples sintered exhibit high dielectric properties, and the dielectric constant reaches about 1.2×10^4 for the LSNO-1 sample. The concentration of Si has a remarkable effect on the dielectric properties of the LSNO ceramics due to the various activation energies corresponding to the dielectric relaxation processes. The experimental results indicate that the polarization relaxation has a close relation with the conductivity in grain interior because the activation energy values, E_g fitted by the reverse temperature dependence of the relaxation time and E_a fitted by the reverse temperature dependence of the dc conductivity, are almost same. The origin of the high permittivity observed in these LSNO ceramics is attributed to the Maxwell-Wagner polarization mechanism and thermally activated mechanism. The calculated dielectric constants by the boundary layer model are in good agreement with the experimental results.

DOI: 10.1103/PhysRevB.72.014103 PACS number(s): 77.22.Ch

I. INTRODUCTION

High-permittivity dielectric materials for their uses in microelectronics such as capacitors and memory devices have been widely investigated, and the dielectric constant will ultimately decide the level of miniaturization.[1,2] The dielectric constant of a material is related to the polarizability, in particular, the dipole polarizability, which arises from structures with a permanent electric dipole. It is well known that oxides with the perovskite structure [e.g., $Pb(Zr,Ti)O_3$, $BaTiO_3$] are used for their high dielectric constants. However, the high dielectric constants always associated with ferroelectric or relaxor properties and exist a peak as a function of temperature due to ferroelectric phase transition.[3,4] Recently, a new perovskite-related material $CaCu_3Ti_4O_{12}$ (CCTO) with an unusually high dielectric constant,[5] which is nearly independent on temperature in the wide temperature range. It was considered that the origin of the large dipole moments in CCTO could be due to the interfacial polarization mechanism, and no ferroelectric transition as in the high-permittivity perovskites has been observed. Additionally, boundary layer capacitors (BLCs) based on semiconductive perovskite oxides, such as $SrTiO_3$, have also been attractive. These BLC ceramics are normally processed in the reductive and partial oxidative atmosphere so that grains of the oxides become semiconducting while grain boundaries are insulating.[6] High-capacitance ceramic capacitors with BLC and MLCC (multilayer ceramic capacitors) structures are the potential trend for attaining high-density charge storage. Raevski *et al.*[7] reported the high dielectric permittivity in nonferroelectric perovskite ceramics (A=Ba, Sr, Ca; B=Nb, Ta, Sb) in a wide temperature interval, and proposed that the phenomenon of the high dielectric permittivity is due to the Maxwell-Wagner relaxation. Generally, the Maxwell-Wagner polarization also known as interfacial polarization was most widely adopted to explain the high permittivity observed in the materials, including single-phase ceramics, single crystals, and multiphase composites, which often arises in a material consisting of grains separated by more insulating intergrain barriers.[8]

In this report, a nonferroelectric and nonperovskite high-permittivity core/shell structured material, $Li_{0.01}Si_xNi_{0.99-x}O$ (abbreviated as LSNO) ceramics, have been successfully synthesized. The high dielectric behavior observed in rocksalt-type LSNO is similar to that observed recently in perovskite-like CCTO. It was suggested that the high dielectric constant response of LSNO could arise from the Maxwell-Wagner polarization (i.e., interfacial polarization) mechanism and thermally activated mechanism such as charge carrier transport rather than due to permanent dipoles.

II. EXPERIMENTAL

$Ni(NO_3)_2\cdot6H_2O$ (A.R.), $LiNO_3$ (A.R.), $Si(C_2H_5O)_4$ (A.R.), and CH_3CH_2OH were employed as raw materials. The specimens with the nominal composition $Li_{0.01}Si_{0.05}Ni_{0.94}O$ (LSNO-1), $Li_{0.01}Si_{0.15}Ni_{0.84}O$ (LSNO-2) and $Li_{0.01}Si_{0.25}Ni_{0.74}O$ (LSNO-3) were prepared by a chemical precipitation combined with solid-state sintering methods. Stoichiometric amounts of $Ni(NO_3)_2\cdot6H_2O$ and $LiNO_3$ were firstly mixed and reacted with $NH_3.H_2O$-NH_4HCO_3 buffer solution to form $Ni_2CO_3(OH)_2$-LiOH composite precipitate. The Ni(Li)O nanosized powders were obtained by the decomposition of the above carbonate precursor and dispersed in CH_3CH_2OH-H_2O solution. Afterwards $Si(C_2H_5O)_4$-CH_3CH_2OH solution was added slowly into the above suspending solution, and then the solution was heated and stirred to form the gel. The amorphous SiO_2/Ni(Li)O coated nanoparticles will be obtained after calcined dried gel. Then the resultant LSNO powders were pressed to green pellets of 10 mm in diameter and about 1.2–1.8 mm in thickness at a pressure of 10 MPa by using polyvinyl alcohol as a binder. Three LSNO ceramic samples were prepared via a

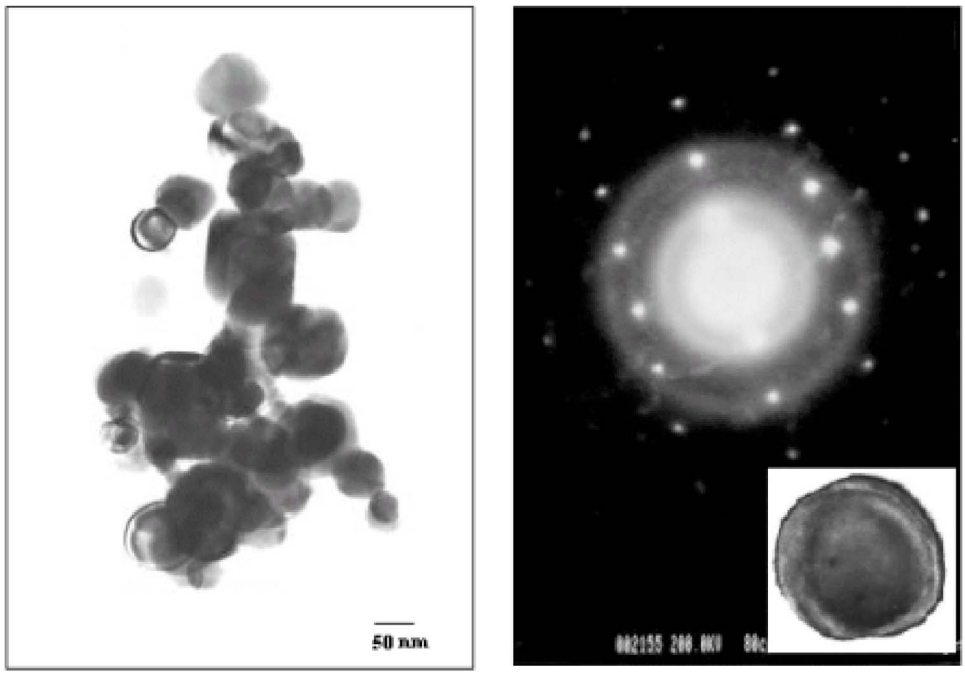

FIG. 1. TEM micrographs and SAED of LSNO-2 precursor particles. (a) TEM micrographs. (b) SAED patterns.

traditional ceramic processing sintered at 1250 °C for 2 h.

X-ray diffraction (XRD), transmission electron microscopy (TEM) with selected area electron diffraction (SAED), scanning electron microscopy (SEM) equipped with energy dispersive spectroscopy (EDS) were employed to reveal microstructure and phase composition of the LSNO ceramics. Dielectric constant measurement was conducted in an evacuated dielectric cell. The dielectric response of the specimens was measured using a HP 4192A gain phase analyzer over a frequency range from 100 Hz to 1 MHz and at an oscillation voltage of 1.0 V.

III. RESULTS AND DISCUSSION

Three kinds of LSNO ceramic samples with the nominal composition $Li_{0.01}Si_{0.05}Ni_{0.94}O$ (LSNO-1), $Li_{0.01}Si_{0.15}Ni_{0.84}O$ (LSNO-2), and $Li_{0.01}Si_{0.25}Ni_{0.74}O$ (LSNO-3) have been synthesized. The original amorphous shell/core structured particles shown in Fig. 1 can be transformed into a grain/grain boundary (GB) structured particles as sintered at 1250 °C for 2 h, and a new Ni_2SiO_4 phase can be observed in the LSNO-2 and LSNO-3 samples. Figures 2 and 3 show the typical microstructure and phase composition of LSNO-2 samples, which implies that the core Ni(Li)O grains have grown to be near 2.0 μm and the dopant of SiO_2 are mainly dispersed into the grain boundaries proved by the EDS results shown in Table I, which probably existed as Ni_2SiO_4 phase in the boundary.

Figure 4 shows the frequency dependence of the dielectric constant ε of the LSNO samples at room temperature. The dielectric constant values at 100 Hz for the LSNO-1, LSNO-2, and LSNO-3 samples are 12375, 6750, and 4964, respectively. The ε value for the LSNO-1 sample is found to be nearly six hundred times larger than that for pure NiO sample.

Figure 5 shows the frequency dependence of the dielectric constant ε (a) and the loss component $\tan\delta$ (b) of the LSNO-1 sample between 10^2 and 10^6 Hz at several temperatures. In Fig. 5(a), the static dielectric constant ε_0 is larger than 10^4, and exhibits a Debye-type variety with increasing frequency. According to Fig. 5(b), there exists a peak correlating to a character relaxation process, and shifts to higher frequency with increasing temperature. The thermally activated behavior are the identifying characteristics of hopping process of polaron conduction, which is confirmed experimentally in *n*-type $BaTiO_3$,[9] $LaMnO_3$,[10] and Ca_2MnO_4.[11] In general, a hopping process of polaron involves a dielectric relaxation process that is described approximately by the De-

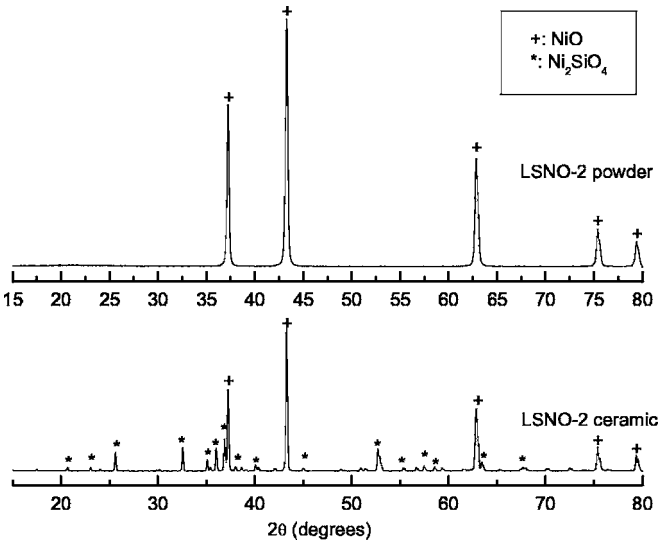

FIG. 2. XRD patterns of LSNO-2 powder and as-sintered products at 1250 °C for 2 h.

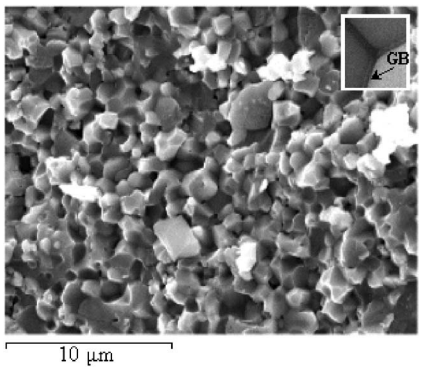

FIG. 3. SEM micrographs of fractured surface for LSNO-2 ceramics.

bye theory.[12] The lower the temperature is, the easier the electric dipoles freeze through the relaxation process. So there exists decay in polarization with respect to the applied electric field, which is evidenced by the dramatic decrease in ε. There are two effects, the rate of polarization formed and the frequency of applied electric field, in determining the relaxation process. When the temperature is high, the rate of polarization formed is quick, and thus the relaxation occur in high frequency as shown in Fig. 5.

Normally, the dielectric relaxation can generally be represented by the following expression[13]

$$\varepsilon(\omega) = \varepsilon_\infty + \frac{\varepsilon_0 - \varepsilon_\infty}{1 - (i\omega\tau)} = \varepsilon'(\omega) + i\varepsilon''(\omega) \tag{1}$$

where ω is the angular frequency, ε_0 and ε_∞ are static dielectric constant ($\omega \to 0$) and permanent dielectric constant ($\omega \to \infty$), respectively, τ is the relaxation time. $\varepsilon'(\omega)$ and $\varepsilon''(\omega)$ are the real and imaginary parts of the dielectric response, respectively, and the loss factor is also referred to as the loss component

$$\tan\delta = \varepsilon''(\omega)/\varepsilon'(\omega) \tag{2}$$

where the angle δ is the phase difference between the applied electric field and the induced current.

As shown in Fig. 5(b), there is the intensive monotonous increase in the loss factor at low frequency, which is probably due to the contribution of the dc conductivity. At low frequency, the ac conductivity is similar to the dc conductivity, so σ_{dc} has an observable influence to the loss component

TABLE I. The results of EDS for the LSNO-2 sample.

	Fractured surface of grain		Grain boundary	
Element	Weight %	Atomic %	Weight %	Atomic %
O	8.79	25.30	15.38	35.68
Si	3.64	5.97	15.70	20.75
Ni	87.58	68.73	68.92	43.57
Si/Ni		0.08		0.48

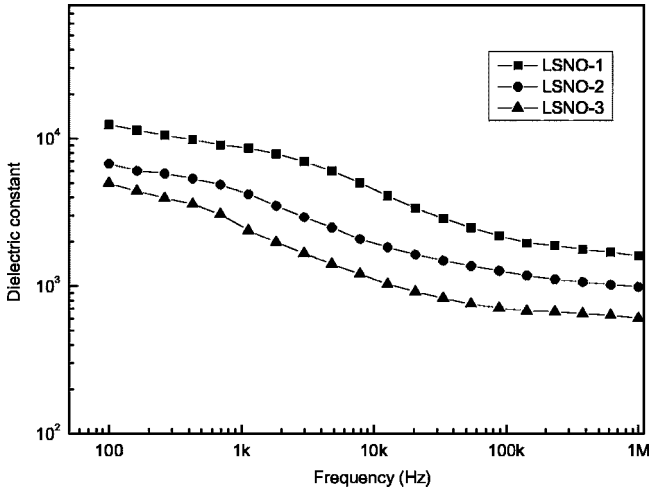

FIG. 4. Frequency dependence of the dielectric constant of the LSNO samples.

of the dielectric response when it is relatively large. With increasing frequency, the influence of the dc conductivity would be ignorable.

According to Eq. (1), $\varepsilon''(\omega) = \omega\tau/1 + (\omega\tau)^2$ and a maximum in $\varepsilon''(T)$ occurs when $\omega\tau = 1$. An Arrhenius plot of the relaxation rate, obtained from the loss and permittivity curves, as a function of inverse temperature is shown in Fig. 6. From this, the rapid decrease of τ with increasing temperature is suggestive of an increasing dipole density and a faster polarization process. The dielectric relaxation time τ should follow:

$$\tau^{-1} = \tau_0^{-1} \exp\left(-E_a/k_B T\right) \tag{3}$$

where E_a is the activation energy required for relaxation, τ_0 represents the pre-exponential factor, and $k_B T$ is the thermal energy.

According to the reverse temperature dependence of the relaxation time τ for different samples, as shown in Fig. 6,

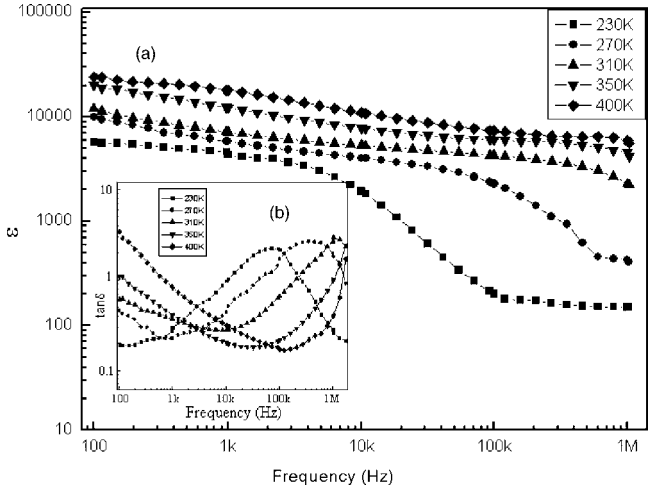

FIG. 5. The frequency dependence of the dielectric constant ε (a) and the loss component $\tan\delta$ (b) of the LSNO-1 sample at various temperatures.

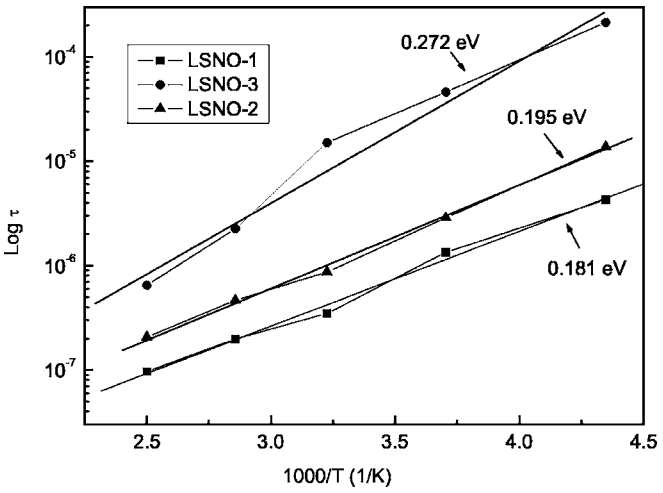

FIG. 6. The reverse temperature dependence of the relaxation time for various samples.

the activity energy E_a of the relaxation process can be obtained, which suggests the activity energy increases with Si concentration (from 0.181 to 0.272 eV).

Conventionally, the relaxations are also dependent on the heterogeneity of the sample. Because the complex impedance spectroscopy is a powerful tool in separating out the bulk and the grain boundary effects, and impedance data on dielectric LSNO ceramics are analyzed using an equivalent circuit consisting of two parallel resistor-capacitor (RC) elements connected in series. In the complex impedance plane plots, a single semicircle indicates the bulk effects and a second semicircle indicates the grain boundary effects. A depressed semicircle, whose center lies on a straight line below the real axis, indicates the departure from ideal Debye-type behavior. The inverse of peak frequency of the semicircle indicates the relaxation time. It can be expressed as the following:[14]

$$Z^* = \frac{R}{(1 + j\omega CR)} = \frac{R}{(1 + j\omega\tau)}, \tag{4}$$

$$\omega_{\max} = \tau^{-1} = (RC)^{-1}. \tag{5}$$

Based on the RC model and the above equation, we can get the R_g, C_g, R_{gb}, and C_{gb} by fitting the curves. Figure 7 shows typical Cole-Cole semicircle for LSNO-2 sample at room temperature. It can be seen that two impedance semicircles exist in this sample, and correspond to the grain and grain boundary. In general, the grain boundary effect on electric conductivity may originate from a grain boundary potential barrier, which could be attributed to the Si-rich boundary (e.g., Ni_2SiO_4).

dc conductivity of NiO is normally considered to be due to the hopping of polarons between localized states. According to the polaron theory, an expression for the temperature dependence of the dc conductivity of modified NiO is, with a temperature-dependent prefactor, given by the following simple equation:[15]

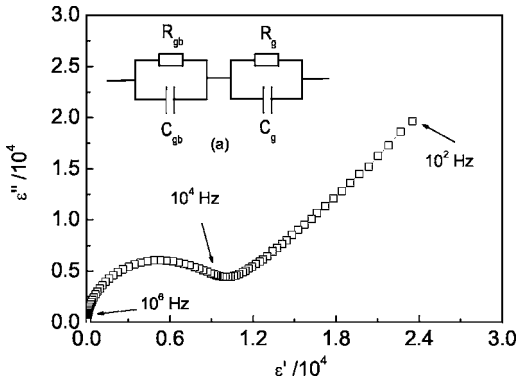

FIG. 7. Typical Cole-Cole semicircle for LSNO-2 sample at room temperature; (a) the RC effective circuit, g and g_b represent grain and grain boundary, respectively.

$$\sigma_{\rm dc} \propto T^{-1} \exp(-W/k_B T) \tag{6}$$

where W, k_B, and T are the activation energy, Boltzmann constant, and absolute temperature, respectively.

Mott and Davis[16] have suggested that an expression for the activation energy W in the small-polaron model as:

$$W = W_H + 1/2 W_D \quad \text{for } T > \Theta_D/2, \tag{6a}$$

$$W \approx W_D \quad \text{for } T < \Theta_D/4. \tag{6b}$$

It implies that the activation energy W in the high-temperature region ($T > \Theta_D/2$) where nearest-neighbor thermally activated hopping predominates results from the polaron-hopping energy (W_H) and the disorder energy (W_D). In the low temperature region ($T < \Theta_D/4$) variable-range hopping takes over from the thermally activated nearest-neighbor hopping and the activation energy is essentially due to disorder energy.

As previously reported, the values of bulk resistance (R_g) and grain boundary resistance (R_{gb}) calculated from the complex impedance plane plots at different temperatures and that from Cole-Cole plots should match.[17] Due to the limitation of our experimental equipment, the data can be available in the temperature range of 230–400 K. Actually, the presence of T^{-1} in the pre-exponential factor of the expression for $\sigma_{\rm dc}$ [Eq. (6)] suggests that the plot of $\lg(\sigma_{\rm dc}T)$ vs T^{-1} should be more appropriate to distinguish the high and low temperature region of dc conduction. As shown in Fig. 8, it can be found that for the semiconducting grain (Li modified NiO core), a deviation from linearity occurs at a temperature $T \sim 320$ K. According to the small-polaron model of hopping conduction, it should take place at a temperature $T = \Theta_D/2$, the fitted activity energies for the grain E_g is about 0.201 eV. However, for the grain boundary, we did not observe this deviation in this temperature range, and the activation energy of grain boundary E_{gb} is about 0.358 eV, which may be attributed to the shell of this structure is great different from the core (e.g., phase composition, defects, etc.), and need the further work for it. As previously reported, doping with Li does not affect the activation energy for electrical conductivity at either very high or very low temperatures.[18] However, in the intermediate temperature range, moderate doping

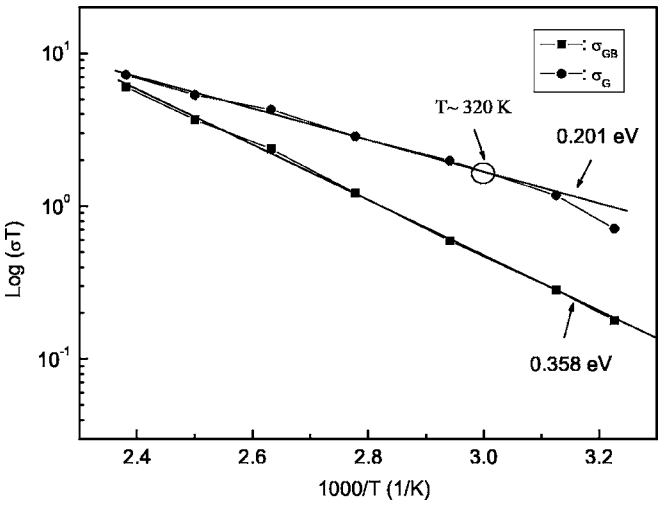

FIG. 8. Typical Arrhenius plots of the conductivities of the grain and the grain boundary of the LSNO-2 sample.

(~1% Li) induces a drop in activation energy from 0.9 eV to about 0.3 eV below 500 K and from 0.6 eV to about 0.2 eV above 500 K. Heavy doping (5%–10% Li) results in a further decrease of activation energy to 0.18 eV below 500 K and 0.14 eV above 500 K.[19] As for our LSNO samples, about 1% Li was doped in the NiO grains, and some additional part of Si are also entered into the NiO grains (indicated by the EDS analysis), which resulted in the grain $E_g \sim 0.201$ eV.

It should be noted that the activation energies E_g (~0.201 eV) of the LSNO-2 sample obtained in Fig. 8 are nearly equal to E_a (~0.195 eV) in Fig. 4 (the activation energy required for relaxation). These experimental results imply that the nature of charge carries responsibility for dielectric relaxation peaks and dc conduction belongs to the same category, which indicates that the polarization relaxation has a close relation with the conductivity in grain interior, and the polarization process probably depends on the conducting of the charge in the grain interior, which result that E_a and E_g are almost same value. The same phenomena are also observed in the other LSNO-2 ($E_g \sim 0.207$ eV and $E_a \sim 0.189$ eV) and LSNO-3 samples ($E_g \sim 0.219$ eV and $E_a \sim 0.198$ eV). In the $BaBiO_3$ system, Lee *et al.* also reported that the E_g is about 0.53 eV for the intermediate temperature region ($294 < T < 230$ K) for the conduction processes, and is nearly equal to the activation energy for polarization relaxation $E_a \sim 0.50$ eV.[20]

Normally, the Maxwell-Wagner polarization, also known as the interfacial polarization, which often arises in a material consisting of grains separated by more insulating intergrain barriers. The Maxwell-Wagner polarization model has been successfully employed to explain the dielectric relaxation with extremely high permittivity ceramics[21] (e.g., CCTO, $BeFe_{1/2}Nb_{1/2}O_3$, $Gd_{0.6}Y_{0.4}BaCo_2O_{5.5}$). The common interpretation assumes a whole series of boundary barriers and grains, or even a series-parallel array of boundary barriers, which arises if the material consists of grains separated by more insulating inter-grain barriers as in boundary layer capacitors.

As previously reported,[22] the resistivity of NiO can be improved by doping monovalent cations several orders of magnitude. The core/shell structured LSNO ceramics consist of the well-conducting grains, Ni(Li)O, and nonconducting or poorly conducting grain boundary layers (e.g., Ni_2SiO_4). Consider grain and grain boundary (GB) having different dielectric permittivities (ε_1 and ε_2) and different conductivities (σ_1 and σ_2), so that the complex permittivities in the LSNO ceramics can be quantitatively approximated by:[23]

$$\varepsilon^* = \frac{L}{d(\varepsilon_1^*)^{-1} + t(\varepsilon_2^*)^{-1}}; \tag{7}$$

here, d is the particle size of conducting grain (core), and t is the thickness of grain boundary (shell), $L=t+d$. Due to $t \ll L$, $\sigma_1 \ll \sigma_2$, Eq. (7) can be simplified as the following:

$$\varepsilon^* = \frac{\varepsilon_1}{\left(1+\frac{d\varepsilon_1}{L\varepsilon_2}\right)} + \frac{\varepsilon_2}{\frac{d}{L}\left(1+\frac{d\varepsilon_1}{L\varepsilon_2}\right)} \times \frac{1}{1+i\omega\tau} = \frac{\varepsilon_1}{\xi} + \frac{\varepsilon_2}{\xi\delta}\frac{1}{1+i\omega\tau} \tag{8}$$

where $\xi = 1+\delta\varepsilon_1/\varepsilon_2$, $\tau = \xi\varepsilon_2/\delta\sigma_1$, $\delta = d/L$.

At zero or very low frequency, the Eq. (8) can be further simplified as:

$$\varepsilon^* = L\varepsilon_2/d. \tag{9}$$

Equation (9) indicates that the dielectric permittivity is controlled by the thin nonconducting layer. As for the LSNO ceramics, the average Ni(Li)O grain size is about 2.0 μm, and the thickness of grain boundary region with increasing doping SiO_2 is estimated to be about 5–15 nm, and the dielectric constant of Ni_2SiO_4 is about 30. Therefore, the dielectric constant at low frequency will be 4000–12 000, which are in good agreement with our experimental data.

IV. CONCLUSIONS

Three kinds of high-permittivity dielectric core/shell structured LSNO ceramics have been successfully prepared by a chemical synthesis combined with the traditional ceramic processing. The dopant of SiO_2 is mainly dispersed into the grain boundaries and exists as the insulating Ni_2SiO_4 phase by EDS and XRD results, which has great influence on the dielectric properties due to the various activation energy, and the dielectric constant varies from 10^3 to 10^4 at low frequency, which is in good agreement with the calculated results by boundary layer model. The high dielectric loss at low frequency is probably caused by the dc conductivity. The high dielectric response can be ascribed to the Maxwell-Wagner polarization mechanism and thermally activated mechanism.

ACKNOWLEDGMENTS

This work was supported by the Ministry of Science and Technology of China through a 973-Project, under Grant No. 2002CB613303; and the National High Technology Research and Development Program of China, under Grant No. 2003AA302120.

[1] S. M. Spearing, Acta Mater. **48**, 179 (2000).
[2] N. Setter and R. Waser, Acta Mater. **48**, 151 (2000).
[3] B. G. Kim, S. M. Cho, T. Y. Kim, and H. M. Jang, Phys. Rev. Lett. **86**, 3404 (2001).
[4] N. A. Pertsev, G. Arlt, A. G. Zembilgotov, Phys. Rev. Lett. **76**, 1364 (1996); H. Haertling, J. Am. Ceram. Soc. **82**, 797 (1999).
[5] M. A. Subramanian, D. Li, N. Duan, B. A. Reisner, and A. W. Sleight, J. Solid State Chem. **151**, 323 (2000). C. C. Homes, T. Vogt, S. M. Shapiro, S. Wakimoto, and A. P. Ramirez, Science **293**, 673 (2001); L. He, J. B. Neaton, M. H. Cohen, D. Vanderbilt, and C. C. Homes, Phys. Rev. B **65**, 214112 (2002); C. C. Homes, T. Vogt, S. M. Shapiro, S. Wakimoto, M. A. Subramanian, and A. P. Ramirez, *ibid.* **67**, 092106 (2003).
[6] C. F. Yang, Jpn. J. Appl. Phys., Part 1 **35**, 1806 (1996); Y. Takeshima, K. Shiratsuyu, H. Takagi, and Y. Sakabe, *ibid.* **36**, 5870 (1997); D. F. K. Hennings, J. Eur. Ceram. Soc. **21**, 1637 (2001).
[7] I. P. Raevski, S. A. Prosandeev, A. S. Bogatin, M. A. Malitskaya, and L. Jastrabik, J. Appl. Phys. **93**, 4130 (2003).
[8] P. Lunkenheimer, V. Bobnar, and A. V. Pronin, Phys. Rev. B **66**, 052105 (2002); Y. H. Lin, J. Wang, L. Jiang, Y. Chen, and C. W. Nan, Appl. Phys. Lett. **85**, 5664 (2004); G. Catalan, D. O'Neill, R. M. Bowman, and J. M. Gregg; *ibid.* **77**, 3078 (2000); J. W. Wu, C. W. Nan, Y. Lin, and Y. Deng, Phys. Rev. Lett. **89**, 217601 (2002).
[9] E. Iguchi, N. Kubota, T. Nakamori, N. Yamamoto, and K. J. Lee, Phys. Rev. B **43**, 8646 (1991).
[10] W. H. Jung, H. Nakatsugawa, and E. Iguchi, J. Solid State Chem. **133**, 466 (1997).
[11] W. H. Jung and E. Iguchi, J. Phys. D **31**, 794 (1998).
[12] L. A. K. Dominik and R. K. MacCrone, Phys. Rev. **163**, 756 (1967); O. Bidault, M. Maglione, M. Actis, M. Kchikech, and B. Salce, Phys. Rev. B **52**, 4191 (1995).
[13] J. Ross Macdonald, *Impedance Spectroscopy* (Wiley, New York, 1987).
[14] J. Liu, C. Duan, W. Yin, W. N. Mei, R. W. Smith, and J. R. Hardy. Phys. Rev. B **70**, 144106 (2004); D. C. Sinclair and A. R. West, J. Appl. Phys. **66**, 3850 (1989).
[15] E. Iguchi and K. Akashi, J. Phys. Soc. Jpn. **61**, 3385 (1992); A. J. Bosman and H. J. van Daal, Adv. Phys. **19**, 1 (1970); P. Pushparajah and S. Radhakrishna, J. Mater. Sci. **32**, 3001 (1997); A. J. Bosman and C. R. Revecoeur, Phys. Rev. **144**, 763 (1965); R. R. Heikes and W. D. Johnston, J. Chem. Phys. **26**, 582 (1957); P. Lunkenheimer, A. Loid, C. R. Ottermann, and K. Bange, Phys. Rev. B **44**, 5927 (1991).
[16] N. F. Mott, J. Non-Cryst. Solids **1**, 1 (1968); N. F. Mott and E. A. Davis, *Electronic Process in Non-Crystalline Materials* (Clarendon, Oxford, 1979).
[17] A. K. Jonscher, *Dielectric Relaxations in Solids* (Chelsea, London, 1983); M. M. Kumar, M. B. Suresh, S. V. Suryanarayana, G. S. Kumar, and T. Bhimasankaram, J. Appl. Phys. **84**, 6811 (1998).
[18] H. J. van Daal and A. J. Bosman, Phys. Rev. **158**, 736 (1967); A. J. Springthorpe, I. G. Austin, and B. A. Austin, Solid State Commun. **3**, 143 (1965); A. David and F. Julius, Phys. Rev. B **2**, 3112 (1970).
[19] S. Koide, J. Phys. Soc. Jpn. **20**, 123 (1965); S. van Houten, Phys. Chem. Solids **17**, 7 (1960).
[20] S. Lee, W. Jung, J. Sohn, J. Lee, and S. Cho, J. Appl. Phys. **86**, 6351 (1999).
[21] Y. Zhi and A. Chen, J. Appl. Phys. **91**, 794 (2002); V. Bobnar, P. Lunkenheimer and M. Paraskevopoulos *et al.*, Phys. Rev. B **65**, 184403 (2002).
[22] V. Biju and M. A. Khadar, J. Mater. Sci. **38**, 4055 (2003).
[23] I. P. Raevski, S. A. Prosandeev, A. S. Bogatin, M. A. Malitskaya, and L. Jastrabik, J. Appl. Phys. **93**, 4130 (2003); C. W. Nan, Prog. Mater. Sci. **37**, 1 (1993).